Ionics (2016) 22:1957–1965
DOI 10.1007/s11581-016-1702-5

ORIGINAL PAPER

Electrochemical response of nitrogen-doped multi-walled carbon nanotubes decorated with gold and iridium nanoparticles toward ferrocyanide/ferricyanide redox system

Nikos G. Tsierkezos[1] · Max Puschner[1] · Uwe Ritter[1] · Andrea Knauer[2] · Lars Hafermann[2] · J. Michael Köhler[2]

Received: 9 March 2016 / Revised: 27 March 2016 / Accepted: 30 March 2016 / Published online: 7 April 2016

Abstract Novel composite films consisting of nitrogen-doped multi-walled carbon nanotubes (N-MWCNTs) were fabricated by means of chemical vapor deposition technique and decorated with gold (AuNP) and iridium (IrNP) nanoparticles possessing diameters of 12.5 and 2.7 nm, respectively. The electrochemical responses of fabricated composite films, further denoted as N-MWCNTs/MNPs (M: Au and Ir), toward ferrocyanide/ferricyanide, $[Fe(CN)_6]^{3-/4-}$ redox couple was probed by means of cyclic voltammetry and electrochemical impedance spectroscopy techniques. The findings demonstrate that both N-MWCNT/MNP composite films exhibit greater electrochemical response and sensitivity toward $[Fe(CN)_6]^{3-/4-}$ compared to unmodified N-MWCNTs. The results verify that the N-MWCNT/MNP composite films are extremely promising for application in electrochemical sensing.

Keywords Electrochemical analysis · Ferrocyanide/ferricyanide · Gold nanoparticles · Iridium nanoparticles · Nitrogen-doped multi-walled carbon nanotubes

Introduction

Sensors based on multi-walled carbon nanotubes (MWCNTs) were extensively applied in electrochemical analysis because of their great electrochemically active area, high electrical conductivity, extremely high reactivity and selectivity, and enhanced chemical stability [1–4]. Furthermore, MWCNTs exhibit improved electric transport properties as well as electrocatalytic properties and are capable to reduce the overpotentials and thereby to improve the currents of redox systems [5–7]. In addition, MWCNTs display high sensitivity and detection capability, and consequently, they improve the reaction rate and amplify the stability and reproducibility of electrode's response [8].

Our research activities were currently involved in fabrication of composite films consisting of MWCNTs and their application in electrochemical analysis [9–13]. In the present manuscript, we report our recent studies on electrochemical response of nitrogen-doped multi-walled carbon nanotubes (N-MWCNTs) modified with gold and iridium nanoparticles, further denoted as N-MWCNTs/MNPs (M: Au and Ir), toward ferrocyanide/ferricyanide, $[Fe(CN)_6]^{3-/4-}$ redox system. The N-MWCNTs were grown direct on oxidized porous silicon wafer upon decomposition of acetonitrile in presence of catalyst and were decorated with AuNPs and IrNPs possessing diameters of 12.5 and 2.7 nm, respectively. In the present manuscript, we are going to demonstrate that the decoration of N-MWCNTs with metal nanoparticles improves significantly their electrocatalytic reactivity and sensitivity.

Experiment

Chemicals and solutions

Potassium hexacyanoferrate(III) (99.0 %), potassium hexacyanoferrate(II) trihydrate (98.5 %), and potassium chloride (99.0 %) were purchased from Sigma-Aldrich, while tetrachloroauric(III) acid trihydrate (>99.5 %) and iridium(III)

✉ Nikos G. Tsierkezos
nikos.tsierkezos@tu-ilmenau.de

[1] Department of Chemistry, Institute of Chemistry and Biotechnology, Ilmenau University of Technology, Ilmenau, Germany

[2] Department of Physical Chemistry and Micro Reaction Technology, Institute of Chemistry and Biotechnology, Ilmenau University of Technology, Ilmenau, Germany

chloride hydrate (>99.9 %) were obtained from Carl Roth GmbH and Alfa Aesar GmbH, respectively. All chemicals were used as received without further purification. For the electrochemistry measurements, a stock solution of $K_3Fe(CN)_6/K_4Fe(CN)_6$ (1.0×10^{-3} mol L^{-1}) was prepared by dissolving appropriate amounts of both compounds in 1.0 mol L^{-1} KCl. The stock solution was prepared immediately prior the electrochemistry measurements using double-distilled water having specific conductivity of 0.50 μS cm^{-1}. The measured solutions in the concentration range of 3.2×10^{-5}–3.2×10^{-4} mol L^{-1} were prepared directly in electrochemical cell with progressive addition of appropriate volume of stock solution in 1.0 mol L^{-1} KCl.

Instrumentation

All electrochemistry measurements were performed on electrochemical working station Zahner (IM6/6EX, Germany). The results were analyzed by means of Thales software (version 4.15). A three-electrode system, consisting of N-MWCNT/MNP (M: Au and Ir) working electrode, platinum auxiliary electrode, and Ag/AgCl (saturated KCl) reference electrode, was used for electrochemistry measurements. The electrochemical impedance spectra were recorded in the frequency range from 0.1 Hz to 100 kHz at the half-wave potential of studied redox system $[Fe(CN)_6]^{3-/4-}$ (0.281 V vs. Ag/AgCl). Details regarding electrochemistry measurements were reported in previous published article [14]. The morphology and elemental composition of N-MWCNT/MNP (M: Au and Ir) composite films were examined using a scanning electron microscope (Zeiss Ultra with an Oxford instruments EDX detector) equipped with an energy dispersive X-ray spectrometer.

Fabrication of N-MWCNT/MNP (M: Au and Ir) composite films

The N-MWCNTs were synthesized by means of chemical vapor deposition technique onto oxidized porous silicon wafer using acetonitrile as carbon and nitrogen source materials in the presence of ferrocene as catalyst [15, 16]. The scheme of pyrolysis apparatus and experimental details were already reported in previous published articles [17–20]. Colloidal noble AuNPs and IrNPs possessing diameters of 12.5 and 2.7 nm, respectively, were fabricated using the photochemical segmented flow technique [21, 22]. A representative scheme of apparatus used for fabrication of MNPs is shown in Fig. 1. The setup was build up of three PC-controlled syringe pumps, PTFE tubing with an inner diameter of 0.5 mm, standard fluid connectors, and one four-port manifold (both made of polyether ether ketone). The segmented flow technique is suitable for microcontinuous-flow synthesis of plasmonic nanoparticles with high size homogeneity and for tuning of nanoparticle properties. It causes a narrow residence time distribution for all volume elements of the reactant mixture under the UV ray and a high reproducibility of the fluid motion in this range. All noble MNPs were prepared using the corresponding metal salt solutions with concentration of 1.0 mM. The salt solution was mixed with the polyvinylpyrrolidone/photoinitiator solution (PVP/PI) in a four-port manifold and segmented with perfluoromethyldecalin (PP9). The PVP/PI solution was previously prepared from PVP solution (2 wt%) and 2-hydroxy-4′-(2-hydroxyethoxy)-2-methylpropiophenone solution (3.0 mM). The nucleation starts with the irradiation of the segments in the photoinitiation element (2 mm length of the focus and irradiation time of 135 ms). The N-MWCNT films were decorated with metal nanoparticles according to following procedure: the N-MWCNT films were immersed in aqueous solution of sodium citrate (2.5 mM) and left in solution for about 10 min. After this treatment, the films were dried in the air for ~2 h at the room temperature. Afterward, the fabricated colloidal solutions of AuNPs and IrNPs were dropped onto treated N-MWCNT films using a micropipette and let for drying under room conditions. Finally, the composite films were carefully washed with distilled water and dried in the air for ~24 h. For the construction of N-MWCNT/MNP (M: Au and Ir) working electrodes, the films were connected to copper wire by using silver conducting coating. Once the silver coating was dried (~24 h), the silver conducting part of films was fully covered with varnish protective coating. Once the protective coating was dried (~12 h), the films were ready to be used as working electrodes for the electrochemistry measurements.

Results and discussion

Scanning electron microscopy analysis of N-MWCNTs/MNPs (M: Au and Ir)

The SEM technique was used to observe directly the morphology of synthesized N-MWCNTs as well as to investigate the surface of N-MWCNT/MNP (M: Au and Ir) composite films. The low-magnification SEM images exhibit that the surface of

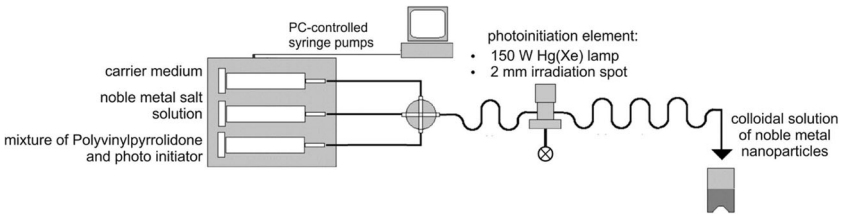

Fig. 1 Scheme of apparatus used for the fabrication of AuNPs and IrNPs

N-MWCNT film is quite homogeneous, and the high-magnification SEM micrographs exhibit that the packing organization, and thus the arrangement of aligned carbon nanotubes on oxidized silicon substrate, is quite enhanced. This observation is attributed to the bamboo-shaped configuration of carbon nanotubes that contain nitrogen incorporated into their structure [23]. The SEM micrographs taken for N-MWCNTs/MNPs reveal that the deposited metal nanoparticles are dispersed homogenously onto the surface of N-MWCNTs and that only slight agglomeration of metal nanoparticles occurs. SEM/EDX analysis of selected AuNPs or IrNPs deposited on N-MWCNTs confirms that these nanoparticles consist of gold and iridium. Representative SEM images taken for N-MWCNT/MNP (M: Au and Ir) composite films are shown in Fig. 2. In these SEM micrographs, the metal nanoparticles can be seen as large bright cyclic particles.

Electrochemical response of N-MWCNTs/MNPs (M: Au and Ir) toward $[Fe(CN)_6]^{3-/4-}$

In order to investigate the effect of metal nanoparticles on electrocatalytic activity of carbon nanotubes, the electrochemical response of N-MWCNT/MNP (M: Au and Ir) composite films toward $[Fe(CN)_6]^{3-/4-}$ redox system (1.0×10^{-3} mol L^{-1}) in aqueous 1.0 M KCl solution was initially tested in large scan rate range (0.02–0.14 V s^{-1}). Representative cyclic voltammetries (CVs) recorded for $[Fe(CN)_6]^{3-/4-}$ on N-MWCNTs/AuNPs at various scan rates are presented in Fig. 3a. For comparison reasons, a CV recorded for 1.0×10^{-3} mol L^{-1} $[Fe(CN)_6]^{3-/4-}$ (1.0 mol L^{-1} KCl) on unmodified N-MWCNT film at the scan rate of 0.02 V s^{-1} is also included in Fig. 3a. The variation of oxidation peak current with the square root of scan rate is shown in Fig. 3b. CVs recorded for $[Fe(CN)_6]^{3-/4-}$ on N-MWCNTs/IrNPs at various scan rates are similar to those obtained for N-MWCNTs/AuNPs and therefore are omitted. The estimated electrochemical parameters $[Fe(CN)_6]^{3-/4-}$ on N-MWCNTs/MNPs (M: Au and Ir) are reported in Table 1. As it can be seen in CVs shown in Fig. 3a, the studied redox system $[Fe(CN)_6]^{3-/4-}$ exhibits a pair of quite reversible redox peaks with anodic and cathodic peak potential separation of $\Delta E_p \approx 0.057$ V ($v = 0.02$ V s^{-1}), which is very close to that expected for one-electron reversible redox process ($\Delta E_p = 0.064$ V), and smaller compared to that obtained on unmodified N-MWCNT film ($\Delta E_p \approx 0.083$ V, $v = 0.02$ V s^{-1}; Fig. 3a) [24]. Consequently, the heterogeneous electron transfer rate constant of $k_s \approx 7.2 \times 10^{-2}$ cm s^{-1}, determined for $[Fe(CN)_6]^{3-/4-}$ on N-MWCNTs/AuNPs by means of electrochemical absolute rate relation [25], appears to be significantly greater compared to that estimated for same redox system on unmodified N-MWCNTs ($k_s \approx 5.1 \times 10^{-3}$ cm s^{-1}) [24]. In addition, the anodic and cathodic peak potential separation of $\Delta E_p \approx 0.066$ V ($v = 0.02$ V s^{-1}) estimated for $[Fe(CN)_6]^{3-/4-}$ on N-MWCNTs/IrNPs appear to be greater compared to N-MWCNTs/AuNPs but nevertheless smaller compared to unmodified N-MWCNTs. Thus, the kinetic parameter of $k_s = 3.8 \times 10^{-2}$ cm s^{-1} estimated for $[Fe(CN)_6]^{3-/4-}$ on N-MWCNTs/IrNPs lies within k_s values obtained for N-

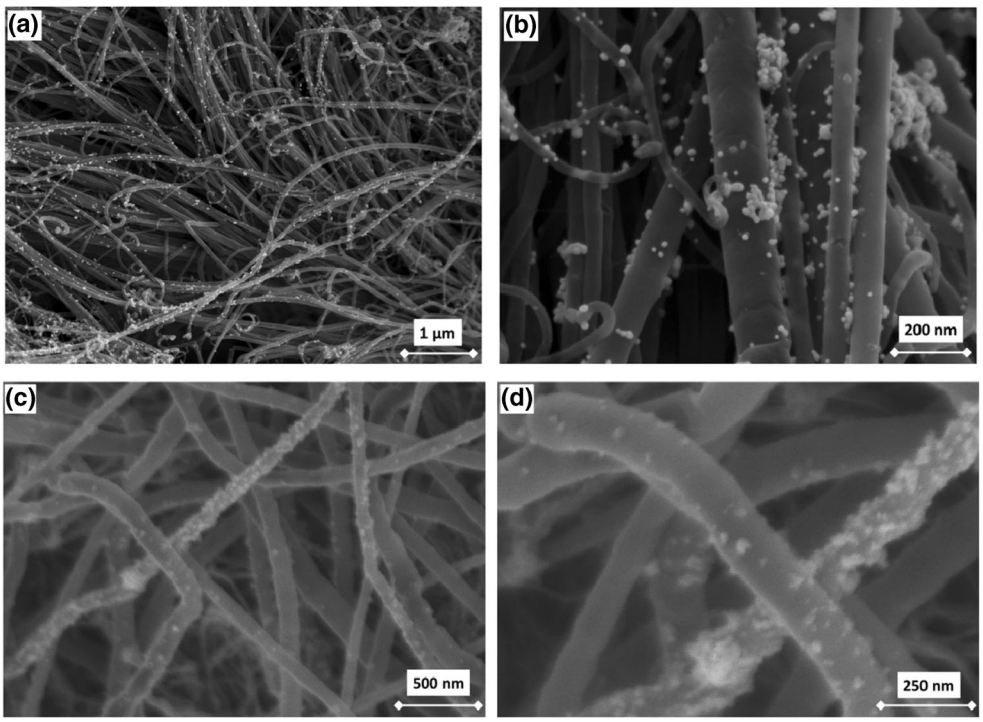

Fig. 2 SEM micrographs of N-MWCNT/AuNP (**a**, **b**) and N-MWCNT/IrNP (**c**, **d**) composite film taken with accelerating voltage of 3 kV and magnification factors of 1.7×10^4 (**a**), 7.6×10^4 (**b**), 4.0×10^4 (**c**), and 10×10^4 (**d**)

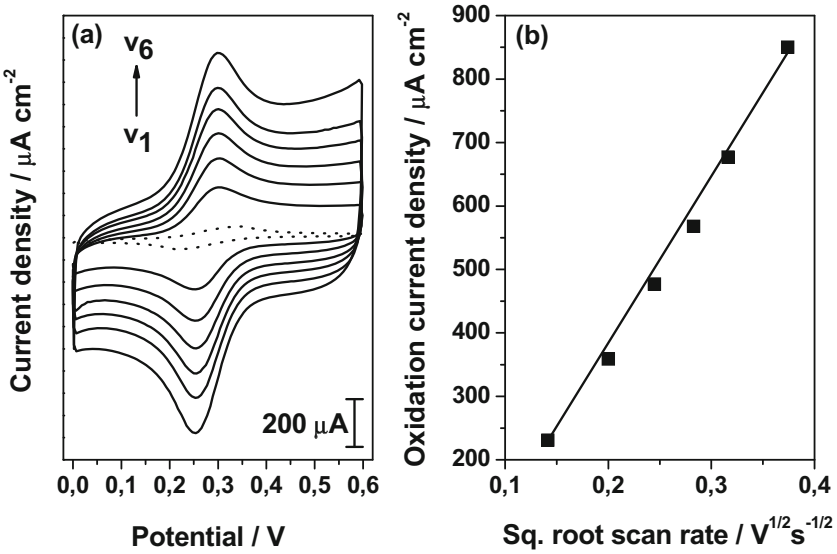

Fig. 3 **a** CVs recorded for 1.0×10^{-3} mol L^{-1} $[Fe(CN)_6]^{3-/4-}$ (1.0 mol L^{-1} KCl) on N-MWCNTs/AuNPs at $v_1 = 0.02$ V s^{-1}, $v_2 = 0.04$ V s^{-1}, $v_3 = 0.06$ V s^{-1}, $v_4 = 0.08$ V s^{-1}, $v_5 = 0.10$ V s^{-1}, and $v_6 = 0.14$ V s^{-1}. CV recorded for 1.0×10^{-3} mol L^{-1} $[Fe(CN)_6]^{3-/4-}$ (1.0 mol L^{-1} KCl) on N-MWCNTs is included (*dotted line*). **b** Variation of oxidation peak current density with square root of scan rate

MWCNTs/AuNPs and N-MWCNTs. The findings exhibit that the modification of N-MWCNTs with metal nanoparticles results to enhanced electrochemical response [26]. However, it must be mentioned that for the determination of k_s of $[Fe(CN)_6]^{3-/4-}$ by means of electrochemical absolute rate relation, the effect of uncompensated resistance was considered as negligible, something that is, in fact, not correct. Namely, the analysis of extracted CV data exhibited concentration

Table 1 Electrochemical parameters determined for $[Fe(CN)_6]^{3-/4-}$ (1.0 M KCl) on N-MWCNT/MNP (M: Au and Ir) films at the scan rate of 0.02 V s^{-1}

Composite film	$E_{1/2}$ (V)	ΔE_p (V)	k_s (cm s^{-1})	R_{ct} (Ω)	*LOD* (μM)	*S* (A M^{-1} cm^{-2})
N-MWCNTs[a]	0.280	0.083	5.1×10^{-3}[c] 6.2×10^{-3}[d]	58	0.341	0.464
N-MWCNTs/AuNPs[b]	0.281	0.057	7.2×10^{-2}[c] 8.0×10^{-2}[d]	2	0.130	0.886
N-MWCNTs/IrNPs[b]	0.282	0.062	3.8×10^{-2}[c] 2.0×10^{-2}[d]	10	0.170	0.752
N-MWCNTs/RhNPs[a]					0.232	0.603
N-MWCNTs/PdNPs[a]					0.185	0.696
N-MWCNTs/PtNPs[a]					0.157	0.766
N-MWCNTs/AgNPs[a]					0.138	0.836
GC/MWCNTs/TiO_2[e]					1.10	
CPE/BMPTFB[f]					100	
CPE/SDS[g]					100	
GCM[h]					30	

Detection limits for other electrode materials reported in literature are also included for comparison reasons [34–37]

[a] Data taken from our previously published article [24]

[b] Data from present work

[c] k_s values determined from electrochemical absolute rate relation, $\psi = (D_o/D_R)^{a/2} k_s(n\pi F v D_o/RT)^{-1/2}$, where ψ is the kinetic parameter, a is the charge transfer coefficient ($a \approx 0.5$), D_o and D_R are the diffusion coefficients of oxidized and reduced species, respectively ($D_o \approx D_R$), and n is the number of electrons involved in the redox reaction ($n = 1$) [32]

[d] k_s values determined from EIS according to relation, $R_{ct} = RT/n^2 F^2 A k_s c$, where R_{ct} is the charge transfer resistance, A is the active surface area, and c is the concentration of redox system [33]

[e] Glassy carbon electrode modified with titanium dioxide and MWCNTs [34] [f] Carbon paste electrode modified with 1-butyl-4-methylpyridinium tetrafluoroborate [35]

[g] Carbon paste electrode modified with sodium dodecyl sulfate [36]

[h] Glass capillary ultra-microelectrode [37]

dependency of ΔE_p, demonstrating that residual uncompensated solution resistance affects the ΔE_p values and consequently the k_s values. Furthermore, it is well known that the electrochemical absolute rate relation is limited to planar diffusion onto flat electrodes, something that is not in agreement with the present work, in which carbon nanotube-based composite film with relative hard and rough surface was used for electrochemistry measurements. Consequently, for better accuracy, the k_s values of $[Fe(CN)_6]^{3-/4-}$ on N-MWCNTs/MNPs (M: Au and Ir) were estimated by means of electrochemical impedance spectroscopy technique and are reported in next paragraphs.

CVs recorded for $[Fe(CN)_6]^{3-/4-}$ on N-MWCNTs/MNPs (M: Au and Ir) exhibit that the peak current ratio of reverse and forward scans is equal to unity and is independent of scan rate, indicating that there are no parallel chemical reactions that are coupled to electrochemical process. Similarly, the oxidative and reductive peak currents are constant for numerous cycles, indicating that there are no chemical reactions coupled to electron transfer process and confirming that $[Fe(CN)_6]^{3-/4-}$ is stable in time frame of experiment and that the charge transfer process occurring on N-MWCNT/MNP (M: Au and Ir) films is reversible. The half-wave potentials of $E_{1/2}$ = 0.281 V (vs. Ag/AgCl) and $E_{1/2}$ = 0.282 (vs. Ag/AgCl) estimated for $[Fe(CN)_6]^{3-/4-}$ redox system on N-MWCNT/AuNP and N-MWCNT/IrNP films, respectively, are similar within experimental error to that measured on unmodified N-MWCNT film ($E_{1/2}$ = 0.280 V vs. Ag/AgCl) [24]. Furthermore, the anodic peak current was found to vary linearly with the square root of scan rate in studied range of 0.02–0.14 V s^{-1}, demonstrating that $[Fe(CN)_6]^{3-/4-}$ is diffusion controlled on N-MWCNTs/MNPs (M: Au and Ir; Fig. 3b). It is very interesting that an improvement of film's current response occurs upon modification of N-MWCNTs with metal nanoparticles. For instance, the current response of N-MWCNTs/AuNPs toward $[Fe(CN)_6]^{3-/4-}$ appears to be around four times greater compared to that of unmodified N-MWCNTs under the same experimental conditions (Fig. 3a). Consequently, it is obvious that the presence of metal nanoparticles onto N-MWCNT film's surface enhances its electrocatalytic activity and improves significantly its electrochemical response. The enhanced electrocatalytic ability of N-MWCNTs/MNPs (M: Au and Ir) is attributed to metal nanoparticles that act as electron antennae that efficiently funnel electrons between the electrode and electrolyte [27].

For the estimation of lower limit of detection of $[Fe(CN)_6]^{3-/4-}$ on N-MWCNTs/MNPs (M: Au and Ir) composite films, CVs for various concentrations of $[Fe(CN)_6]^{3-/4-}$ in concentration range from ~3.0 × 10^{-5} to ~3.0 × 10^{-4} mol L^{-1} were recorded at the scan rate of 0.02 V s^{-1} (Figs. 4a and 5a). The electrochemical response of N-MWCNTs/MNPs (M: Au and Ir) toward $[Fe(CN)_6]^{3-/4-}$ plotted as oxidation peak current density vs. concentration of electroactive compound appears to be linear in investigated concentration range (Figs. 4b and 5b). From the linear concentration-current calibration curve, the detection limit and sensitivity values of 0.130 μM and 0.886 A M^{-1} cm^{-2}, respectively, were estimated for N-MWCNTs/AuNPs toward $[Fe(CN)_6]^{3-/4-}$. With similar manner, the detection limit and sensitivity values of 0.170 μM and 0.752 A M^{-1} cm^{-2}, respectively, were obtained for N-MWCNTs/IrNPs toward $[Fe(CN)_6]^{3-/4-}$. These values are compared with those obtained for unmodified N-MWCNT film as well as for other novel composite films reported in literature in Table 1. From this comparison, it can be clearly seen that the detection ability and sensitivity of N-MWCNTs enhance significantly upon modification with metal nanoparticles. In addition, our novel N-MWCNT/AuNP film exhibits slightly greater detection ability toward $[Fe(CN)_6]^{3-/4-}$

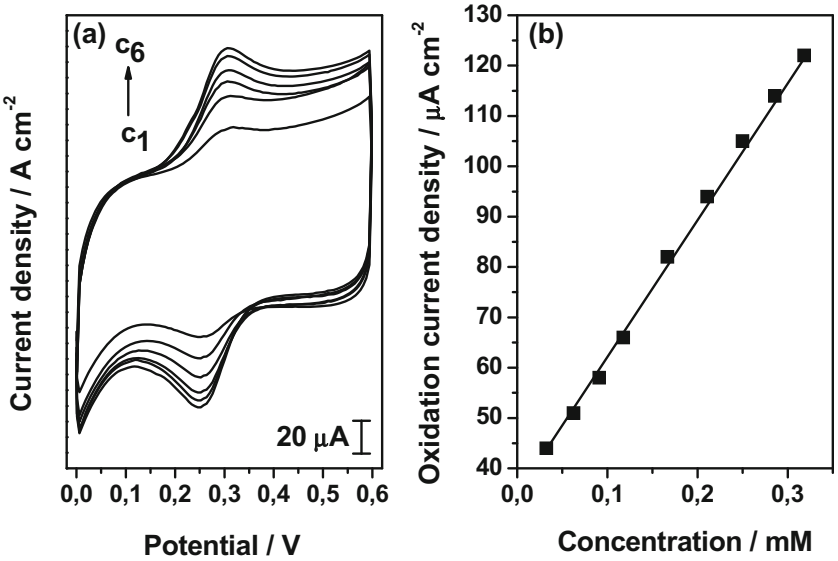

Fig. 4 **a** CVs recorded on N-MWCNTs/AuNPs for $c_1 = 1.18 \times 10^{-4}$ mol L^{-1}, $c_2 = 1.67 \times 10^{-4}$ mol L^{-1}, $c_3 = 2.11 \times 10^{-4}$ mol L^{-1}, $c_4 = 2.50 \times 10^{-4}$ mol L^{-1}, $c_5 = 2.86 \times 10^{-4}$ mol L^{-1}, and $c_6 = 3.18 \times 10^{-4}$ mol L^{-1} $[Fe(CN)_6]^{3-/4-}$ (1.0 mol L^{-1} KCl) at v = 0.02 V s^{-1}. **b** Variation of oxidation peak current density with concentration of $[Fe(CN)_6]^{3-/4-}$

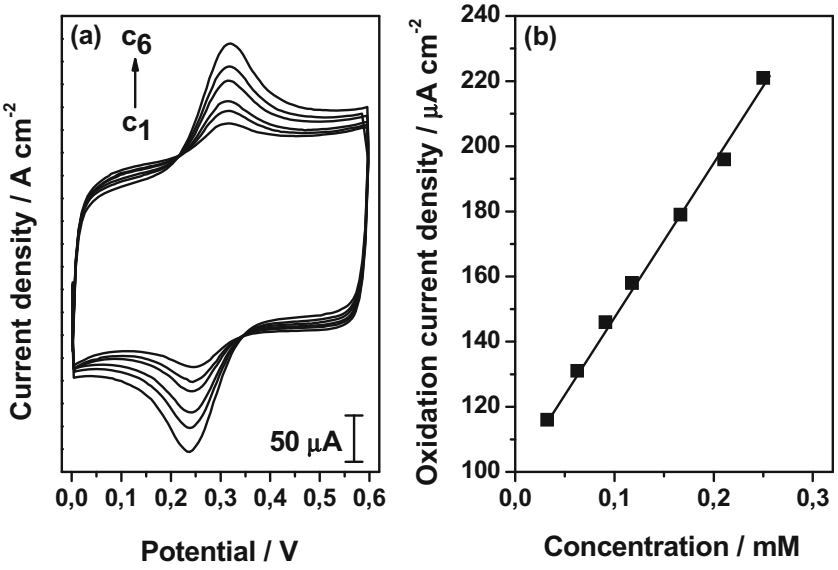

Fig. 5 **a** CVs recorded on N-MWCNTs/IrNPs for $c_1 = 6.25 \times 10^{-5}$ mol L^{-1}, $c_2 = 9.09 \times 10^{-5}$ mol L^{-1}, $c_3 = 1.18 \times 10^{-4}$ mol L^{-1}, $c_4 = 1.67 \times 10^{-4}$ mol L^{-1}, $c_5 = 2.11 \times 10^{-4}$ mol L^{-1}, and $c_6 = 2.50 \times 10^{-4}$ mol L^{-1} $[Fe(CN)_6]^{3-/4-}$ (1.0 mol L^{-1} KCl) at $v = 0.05$ V s^{-1}. **b** Variation of oxidation peak current density with concentration of $[Fe(CN)_6]^{3-/4-}$

compared to N-MWCNTs/IrNPs. Moreover, both novel N-MWCNTs/MNPs (M: Au and Ir) demonstrate significantly enhanced response toward $[Fe(CN)_6]^{3-/4-}$ compared to other novel electrode materials reported in literature (Table 1).

It would be very interesting to compare the lower limit of detection of N-MWCNTs/MNPs (M: Au and Ir) toward $[Fe(CN)_6]^{3-/4-}$ with those estimated for N-MWCNTs modified with other metal nanoparticles, such as RhNPs, PdNPs, PtNPs, and AgNPs, previously published in literature [24]. Consequently, the detection limit of N-MWCNTs/MNPs (M: Au and Ir) toward $[Fe(CN)_6]^{3-/4-}$ is presented graphically along with those reported in literature for N-MWCNTs/RhNPs [24], N-MWCNTs/PdNPs [24], N-MWCNTs/PtNPs [24], and N-MWCNTs/AgNPs [24] in histogram in Fig. 6a. From this comparison, it can be clearly seen that the lower limit of detection of composite films toward $[Fe(CN)_6]^{3-/4-}$ decreases with the following order: N-MWCNTs/RhNPs > N-MWCNTs/PdNPs > N-MWCNTs/IrNPs > N-MWCNTs/PtNPs > N-MWCNTs/AgNPs > N-MWCNTs/AuNPs. These findings exhibit the greater ability of AuNPs to improve the sensitivity and electrocatalytic activity of N-MWCNTs. A correlation of lower limit of detection of modified N-MWCNTs/MNPs (where M: Au, Ir, Rh, Pd, Pt, and Ag) films with the electron density of corresponding metal nanoparticles can be also extracted. Figure 6b displays the dependence of lower limits of detection of N-MWCNTs/AuNPs, N-MWCNTs/IrNPs, N-MWCNTs/RhNPs, N-MWCNTs/PdNPs, N-MWCNTs/PtNPs, and N-MWCNTs/AgNPs toward $[Fe(CN)_6]^{3-/4-}$ on energy of onset of density of electron state (DOS) of corresponding metal nanoparticles reported in literature by Smith et al. [28, 29]. It must be mentioned that the onset energies of DOS were calculated from the model band structures and the zero of energy corresponds to the Fermi level. In Fig. 6b, it can be clearly seen that the detection ability,

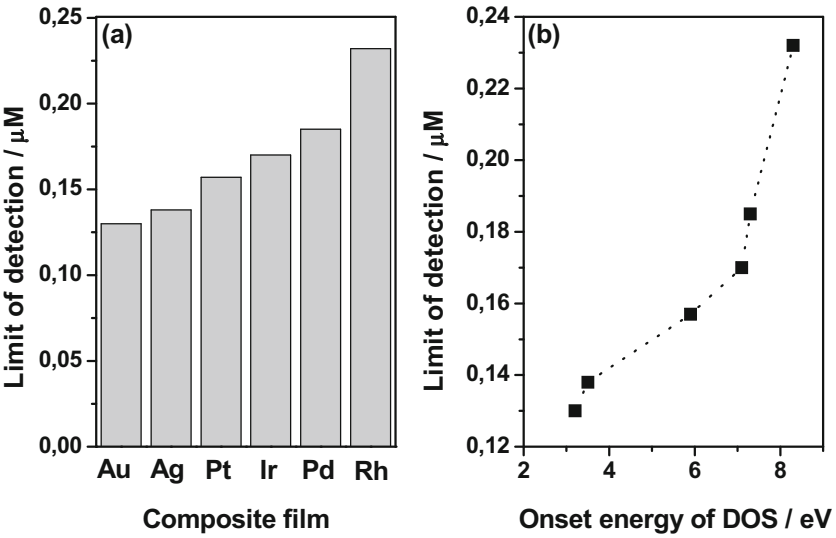

Fig. 6 **a** Histogram demonstrating the limit of detection of N-MWCNTs/RhNPs [24], N-MWCNTs/PdNPs [24], N-MWCNTs/PtNPs [24], N-MWCNTs/AgNPs [24], N-MWCNTs/AuNPs, and N-MWCNTs/IrNPs toward $[Fe(CN)_6]^{3-/4-}$ (1.0 mol L^{-1} KCl). **b** *Diagram* showing the limit of detection of N-MWCNTs/RhNPs [24], N-MWCNTs/PdNPs [24], N-MWCNTs/PtNPs [24], N-MWCNTs/AgNPs [24], N-MWCNTs/AuNPs, and N-MWCNTs/IrNPs toward $[Fe(CN)_6]^{3-/4-}$ (1.0 mol L^{-1} KCl) vs. onset energy of DOS of metal nanoparticles [28, 29]

and thus the sensitivity of composite film, is related to onset energy of DOS of metal nanoparticles. Namely, there is a trend of decreasing of detection limit with the decrease of onset energy of DOS. Thus, the smallest onset energy of DOS of AuNPs (3.2 eV) leads to the lowest detection limit (the greatest sensitivity), while the greatest onset energy of DOS of RhNPs (8.3 eV) results to the highest detection limit (the lowest sensitivity).

The electrochemical behavior of $[Fe(CN)_6]^{3-/4-}$ redox system on N-MWCNTs/MNPs (M: Au and Ir) was further investigated by means of electrochemical impedance spectroscopy technique. Namely, EIS spectra were recorded for $[Fe(CN)_6]^{3-/4-}$ redox system on N-MWCNT/MNP (M: Au and Ir) composite films at the half-wave potential studied redox system (0.281 V vs. Ag/AgCl) in the frequency range of 0.1 Hz–100 kHz. Representative EIS spectra recorded for 1.0×10^{-3} mol L^{-1} $[Fe(CN)_6]^{3-/4-}$ (1.0 mol L^{-1} KCl) on N-MWCNTs/MNPs (M: Au and Ir) are shown in Fig. 7. The EIS spectra were simulated by means of Nyquist circuit for estimating the charge transfer resistance, which is parameter that controls the electron transfer kinetics of redox system at electrode interface and represents the barrier for electron transfer (the hindering behavior of interface properties of electrode) [30]. The Nyquist circuit, which can represented as (R_s + (C_{dl}/(R_{ct} + Z_w))), consists of solution resistance (R_s), double-layer capacitance (C_{dl}) (constant phase element was used instead of capacitor), charge transfer resistance (R_{ct}), and Warburg diffusion impedance (Z_w) (inset in Fig. 7). The estimated R_{ct} values for $[Fe(CN)_6]^{3-/4-}$ on N-MWCNTs/MNPs (M: Au and Ir) are included in Table 1 along with that obtained for $[Fe(CN)_6]^{3-/4-}$ on unmodified N-MWCNTs [24]. The findings demonstrate that the modification of N-MWCNTs with metal nanoparticles leads to lower charge transfer resistance, and thus to less barrier for electron transfer, resulting therefore to faster kinetics of redox process occurring on these particular films (it is well known that the heterogeneous charge transfer rate varies inversely with charge transfer resistance) [31]. Namely, upon modification of N-MWCNTs with AuNPs and IrNPs, the charge transfer resistance decreases for about ~90 and ~80 %, respectively, resulting to an improvement of kinetic of electrochemical process. For better accuracy, the kinetic parameter k_s was estimated using the charge transfer resistance obtained by means of electrochemical impedance spectroscopy. As was expected, significantly greater k_s values of $[Fe(CN)_6]^{3-/4-}$ were estimated on N-MWCNT/AuNP ($k_s \approx 8.0 \times 10^{-2}$ cm s^{-1}) and N-MWCNT/IrNP ($k_s \approx 2.0 \times 10^{-2}$ cm s^{-1}) films compared to that determined on unmodified N-MWCNTs ($k_s \approx 6.2 \times 10^{-3}$ cm s^{-1}) [24]. This finding demonstrates the greater electrocatalytic activity of N-MWCNTs modified with metal nanopartices. It is also obvious that the kinetic of $[Fe(CN)_6]^{3-/4-}$ redox system on N-MWCNTs/AuNPs appears to be faster compared to that on N-MWCNTs/IrNPs. Furthermore, the k_s values determined from charge transfer resistance differ slightly with those estimated by means of electrochemical absolute rate relation. This disagreement is attributed to the greater inaccuracy of calculating k_s by means of absolute rate relation since the uncompensated resistance effect is not negligible. Considering that k_s calculated by means of impedance spectroscopy is more truthful compared to that estimated by means of electrochemical absolute rate relation, it can be concluded that the kinetics of $[Fe(CN)_6]^{3-/4-}$ on N-MWCNTs/AuNPs is more than 10 times faster compared to that on unmodified N-MWCNTs and about 4 times faster compared to that on N-MWCNTs/IrNPs. It is obvious that the decoration of N-MWCNTs with metal nanoparticles results to lower barrier for electron transfer and therefore, to faster kinetics of redox process occurring on composite film. The extracted results exhibit the importance of modifying N-MWCNTs with metal nanoparticles (especially AuNPs) for the improvement of their electrocatalytic activity.

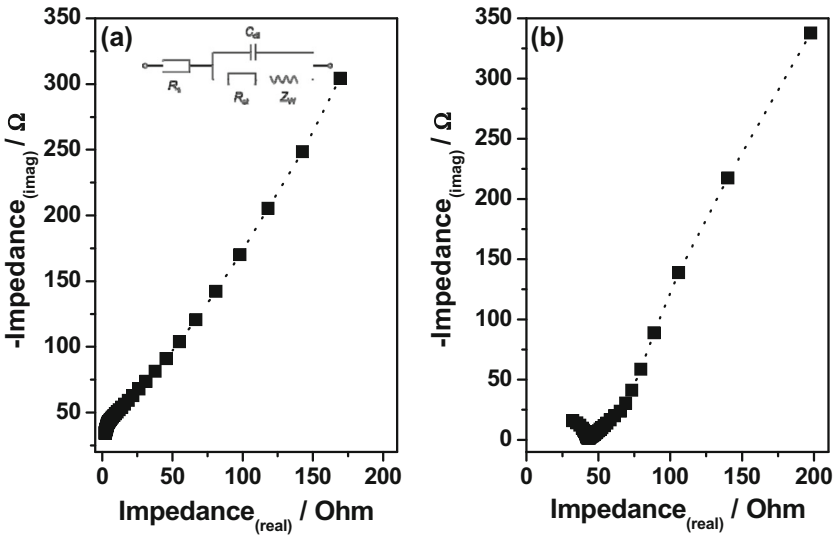

Fig. 7 EIS recorded for 1.0×10^{-3} mol L^{-1} $[Fe(CN)_6]^{3-/4-}$ (1.0 mol L^{-1} KCl) on N-MWCNTs/AuNPs (**a**) and N-MWCNTs/IrNPs (**b**) at the potential of 0.281 V (vs. Ag/AgCl) in the frequency range of 0.1 Hz–100 kHz. *Inset* is equivalent electrical circuit (R_s + (C_{dl}/(R_{ct} + Z_w))) used for simulation of EIS spectra (software Thales, version 4.15)

The repeatability and reproducibility of N-MWCNT/MNP (M: Au and Ir) composite films were evaluated by means of CV technique. The reproducibility of method was studied by measuring the electrochemical response of five different N-MWCNT/MNP (M: Au and Ir) films toward $[Fe(CN)_6]^{3-/4-}$. In all cases, the reproducibility was estimated in the range of 2.5–3.5 %. Furthermore, the repeatability of the method was studied by monitoring the current response of the same N-MWCNT/MNP (M: Au and Ir) film toward $[Fe(CN)_6]^{3-/4-}$ for 10 different successive measurements. The repeatability of less than 3.0 % estimated for N-MWCNT/MNP (M: Au and Ir) composite films can be considered quite acceptable. These findings demonstrate that N-MWCNT/MNP (M: Au and Ir) films have quite good repeatability and reproducibility toward $[Fe(CN)_6]^{3-/4-}$.

Conclusions

The electrochemical response of N-MWCNTs/MNPs (M: Au and Ir) toward $[Fe(CN)_6]^{3-/4-}$ was investigated in aqueous KCl solution in large scan rate and concentration ranges. The findings demonstrate that $[Fe(CN)_6]^{3-/4-}$ appears to be reversible and diffusion controlled on N-MWCNT/MNP (M: Au and Ir) composite films. The electrode's electrochemical response as well as the kinetic of electron transfer for $[Fe(CN)_6]^{3-/4-}$ become significantly faster upon modification of N-MWCNTs with metal nanoparticles. In addition, the detection ability of decorated N-MWCNTs/MNPs (M: Au and Ir) toward $[Fe(CN)_6]^{3-/4-}$ appears to be more than two times greater compared to that of unmodified N-MWCNTs. The results of present work demonstrate the improvement of sensitivity and electrocatalytic activity of N-MWCNTs upon modification with metal nanoparticles.

Acknowledgments The authors would like to thank Mrs. Doreen Schneider (Ilmenau University of Technology). The authors gratefully acknowledge the funding from BMBF (project "BactoCat" Kz 031A161A) as well as the funding from DFG (project KO-1406/39-1).

References

1. Ranganathan S, Kuo T, McCreery RL (1999) Facile preparation of active glassy carbon electrodes with activated carbon and organic solvents. Anal Chem 71:3574–3580
2. Prylutska SV, Grynyuk II, Matyshevska OP, Yashchuk VM, Prylutskyy YI, Ritter U, Scharff P (2008) Estimation of multi-walled carb on nanotubes toxicity in vitro. Phys E 40:2565–2569
3. Burlaka A, Lukin S, Prylutska S, Remeniak O, Yu P, Shuba M, Maksimenko S, Ritter U, Scharff P (2010) Hyperthermic effect of multi-walled carbon nanotubes stimulated with near infrared irradiation for anticancer therapy: in vitro studies. Exp Oncol 32:48–50
4. Grechnev GE, Desnenko VA, Fedorchenko AV, Panfilov AS, Matzui LY, Prylutskyy YI, Grybova MI, Ritter U, Scharff P, Kolesnichenko YA (2010) Structure and magnetic properties of multi-walled carbon nanotubes modified with iron. Low Temp Phys 36:1086–1090
5. Sherigara BS, Kutner W, D'Souza F (2003) Electrocatalytic properties and sensor applications of fullerenes and carbon nanotubes. Electroanalysis 15:753–772
6. Matzui LY, Ovsienko IV, Len TA, Prylutskyy YI, Scharff P (2005) Transport properties of composites with carbon nanotube-based composites. Fullerenes Nanotubes Carbon Nanostruct 13:259–265
7. Ovsienko V, Len TA, Matzui LY, Prylutskyy YI, Ritter U, Scharff P, Le Normand F, Eklund P (2007) Resistance of nanocarbon material containing nanotubes. Mol Cryst Liq Cryst 468:289–297
8. Yun YH, Dong Z, Shanov V, Heineman WR, Halsall HB, Bhattacharya A, Conforti L, Narayan RK, Ball WS, Schulz MJ (2007) Nanotube electrodes and biosensors. Nano Today 2:30–37
9. Tsierkezos NG, Ritter U (2010) Synthesis and electrochemistry of multi-walled carbon nanotube films directly attached on silica substrate. J Solid State Electrochem 14:1101–1107
10. Tsierkezos NG, Ritter U, Philippopoulos AI, Schröder D (2010) Electrochemical studies of the bis(triphenyl phosphine) ruthenium(II) complex, *cis*-$[RuCl_2(L)(PPh_3)_2]$, with L = 2-(2′-pyridyl)quinoxaline. J Coord Chem 63:3517–3530
11. Tsierkezos NG, Ritter U (2011) Determination of impedance spectroscopic behavior of triphenylphosphine on various electrodes. Anal Lett 44:1416–1430
12. Tsierkezos NG, Ritter U (2012) Simultaneous detection of ascorbic acid and uric acid at MWCNT modified electrodes. J Nanosci Lett 2:25
13. Tsierkezos NG, Wetzold N, Ritter U (2013) Electrochemical responses of carbon nanotubes-based films printed on polymer substances. Ionics 19:335–341
14. Tsierkezos NG, Philippopoulos AI, Ritter U (2010) Electrochemical impedance spectroscopy and cyclic voltammetry of *cis*-$[Cr(bipy)_2(SCN)_2]I$ (where bipy: 2,2′-bipyridine) in polar solvents. J Solut Chem 39:897–908
15. Rao CNR, Sen R (1998) Large aligned-nanotube bundles from ferrocene pyrolysis. Chem Commun 1525–1526
16. Ovsienko IV, Len TA, Matsuy LY, Prylutskyy YI, Andrievskiy VV, Berkutov IB, Mirzoiev IG, Komnik YF, Grechnev GE, Kolesnichenko YA, Hayn R, Scharff P (2015) Magnetoresistance and electrical resistivity of N-doped multi-walled carbon nanotubes at low temperatures. Phys St Sol (b) 252:1402–1409
17. Szroeder P, Tsierkezos NG, Scharff P, Ritter U (2010) Electrocatalytic properties of carbon nanotube carpets grown on Si-wafers. Carbon 48:4489–4496
18. Tsierkezos NG, Ritter U (2010) Electrochemical impedance spectroscopy and cyclic voltammetry of ferrocene in acetonitrile/acetone system. J Appl Electrochem 40:409–417
19. Tsierkezos NG, Szroeder P, Ritter U (2011) Application of films consisting of carbon nanoparticles for electrochemical detection of redox systems in organic solvent media. Fullerenes Nanotubes Carbon Nanostruct 19:505–516
20. Tsierkezos NG, Rathsmann E, Ritter U (2011) Electrochemistry on multi-walled carbon nanotubes in organic solutions. J Solut Chem 40:1645–1656
21. Köhler JM, Li S, Knauer A (2013) Why is micro segmented flow particularly promising for the synthesis of nanomaterials. Chem Eng Technol 36:887–899
22. Hafermann L, Köhler JM (2015) Photochemical micro continuous-flow synthesis of noble metal nanoparticles of the platinum group. Chem Eng Technol 38:1138–1143
23. Katayama T, Araki H, Yoshino K (2002) Multi-walled carbon nanotubes with bamboo-like structure and effects of heat treatment. J Appl Phys 91:6675–6678
24. Tsierkezos NG, Haj Othman S, Ritter U, Hafermann L, Knauer A, Köhler JM (2014) Nitrogen-doped multi-walled carbon nanotubes

modified with platinum, palladium, rhodium and silver nanoparticles in electrochemical sensing. J Nanoparticle Res 16:2660
25. Nicholson RS (1965) Theory and application of cyclic voltammetry for measurement of electrode reaction kinetics. Anal Chem 37: 1351–1355
26. Li X, Ren T, Wang N, Ji X (2013) Gold nanoparticles-enhanced amperometric tyrosinase biosensor based on three-dimensional sol-gel film-modified gold electrodes. Anal Sci 29:473–477
27. Guo Y, Guo S, Fang Y, Dong S (2010) Gold nanoparticle/carbon nanotube hybrids as an enhanced material for sensitive amperometric determination of tryptophan. Electrochim Acta 55:3927–3931
28. Smith NV (1974) Photoemission spectra and band structures of d-band metals. III. model band calculations on Rh, Pd, Ag, Ir, Pt, and Au. Phys Rev B 9:1365–1376
29. Smith NV, Wertheim GK, Hüfner S, Traum MM (1974) Photoemission spectra and band structures of d-band metals. X-ray photoemission spectra and densities of states in Rh, Pd, Ag, Ir, Pt, and Au. Phys Rev B 10:3197–3206
30. Esplandiu MJ, Pacios M, Bellido E, Del Valle M (2007) Carbon nanotubes and electrochemistry. Z Phys Chem 221:1161–1173
31. Tsierkezos NG, Szroeder P, Ritter U (2011) Multi-walled carbon nanotubes as electrode materials for electrochemical studies of organometallic compounds in organic solvent media. Monatsh Chem 142:233–242
32. Brett CMA, Brett AMO (1998) Electroanalysis. Oxford University Press Inc., New York
33. Galus Z (1994) Fundamentals of electrochemical analysis. Ellis Horwood, New York
34. Perenlei G, Tee TW, Yusof NA, Kheng GJ (2011) Voltammetric detection of potassium ferricyanide mediated by multi-walled carbon nanotube/titanium dioxide composite modified glassy carbon electrode. Int J Electrochem Sci 6:520–531
35. Pandurangachar M, Swamy BEK, Chandrashekar BN, Gilbert O, Reddy S, Sherigara BS (2010) Electrochemical investigations of potassium ferricyanide and dopamine by 1-butyl-4-methylpyridinium tetrafluoroborate modified carbon paste electrode: a cyclic voltammetric study. Int J Electrochem Sci 5:1187–1202
36. Niranjana E, Swamy BEK, Naik RR, Sherigara BS, Jayadevappa H (2009) Electrochemical investigations of potassium ferricyanide and dopamine by sodium dodecyl sulphate modified carbon paste electrode: a cyclic voltammetric study. J Electroanal Chem 631:1–9
37. Hirano A, Kanai M, Nara T, Sugawara M (2001) A glass capillary ultramicroelectrode with an electrokinetic sampling ability. Anal Sci 17:37–43